

ON THE STABILITY OF A STEADY CONVECTIVE FLOW IN A VERTICAL LAYER OF A CHEMICALLY REACTING FLUID

ARMANDS GRITSANS*, VALENTINA KOLISKINA[†], ANDREI
KOLYSHKIN[†], AND FELIX SADYRBAEV*

*Department of Physics and Mathematics
Daugavpils University
1 Parades street, Daugavpils, LV5401, Latvia
e-mail: armands.gricans@du.lv, felix@latnet.lv

[†]Department of Engineering Mathematics
Riga Technical University
2 Daugavgrivas street, Riga, LV1007, Latvia
e-mail: valentina.koliskina@rtu.lv, andrejs.koliskins@rtu.lv

Key words: Nonlinear Heat Sources, Bifurcation Analysis, Boundary Value Problem, Linear Stability

Abstract. Linear stability of a steady flow of a chemically reacting fluid located in a vertical fluid layer bounded by two infinite parallel planes is investigated. Steady convective flow in the vertical direction is initiated due to the combined effect of internal heat generation and the temperature difference between the planes. Imposing small perturbations on the base flow, linearizing equations of thermal convection under the Boussinesq approximation in the neighbourhood of the base flow and using the method of normal modes we obtain an eigenvalue problem for a system of ordinary differential equations. Collocation method is used to discretize the problem. Numerical calculations are performed in Matlab. Fluid velocity, pressure, and temperature are the solutions of a nonlinear boundary value problem. Properties of the nonlinear boundary value problem for the base flow are investigated numerically using bifurcation analysis. It is shown that both the temperature difference between the planes and intensity of internal heat generation have a destabilizing influence on the base flow. The intensity of heat transfer in the direction perpendicular to the main flow can promote instability and leads to more intensive mixing. This fact can be used in design of bioreactors for biomass thermal conversion.

1 INTRODUCTION

Development of our society in the near future will be dependent on the availability of alternative sources of energy. One promising area of investigation is biomass thermal conversion [1, 2]. Researchers try to understand experimentally the importance of different factors (such as applied electrical field, intensity of chemical reactions, fluid mixing) on the efficiency of the conversion process [3, 4]. Alternative approach is based on numerical modeling [5]. Biomass thermal conversion is described by complex interaction of the following processes: combustion, heat transfer, and fluid flow. One popular method of investigation of complex processes in fluid mechanics is stability analysis [6, 7]. Stability of convective flows is a topic of continuous interest due to numerous applications in physics and engineering. In some cases (biomass thermal conversion is one example) instability is desired since it results in more intensive mixing and (possibly) in more efficient energy conversion. Linear stability analysis of a steady convective flow due to internal heat generation in a vertical fluid layer is analyzed in [7]. Stability of a stationary flow in an annulus in the presence of a nonlinear heat source is analyzed in [8]. In the present paper we consider a linear stability problem that takes into account heat generated in the fluid as a result of chemical reaction and the temperature difference across the fluid layer.

2 MATHEMATICAL FORMULATION OF THE PROBLEM

Chemical reactions occurring in the fluid generate heat and new components. Changes in temperature and concentration lead to a non-uniform density. As a result, convective flows are developed. If thermal effect of the reaction is large enough we can neglect the dependence of the generated heat on the concentration of the components. Convection is then generated due to internal heat sources distributed within the fluid in accordance with the Arrhenius' law:

$$Q = Q_0 \exp\left(-\frac{E}{RT}\right), \quad (1)$$

where T is the temperature, R is the universal gas constant and E is the parameter characterizing reaction.

Consider an infinitely long vertical fluid layer filled with viscous incompressible fluid. The walls $\tilde{x} = \pm h$ are maintained at constant temperatures \hat{T} and $-\hat{T}$, respectively. We let the measures of length, time, velocity, temperature and pressure be h , h^2/ν , $\hat{g}\hat{\beta}h^2\hat{T}/(\nu E)$, $R\hat{T}^2/E$, $\rho\hat{g}\hat{\beta}hR\hat{T}^2/E$, respectively. Here ρ is the density, $\hat{\beta}$ is the coefficient of thermal expansion, \hat{g} is the acceleration due to gravity and ν is the kinematic viscosity. Let (x, y, z) be a system of Cartesian coordinates whose origin lies in the middle of the two planes $\tilde{x} = \pm h$ and the z -axis is directed upwards. The flow is described by the

system of equations of thermal convection under the Boussinesq approximation:

$$\frac{\partial \mathbf{v}}{\partial t} + Gr(\mathbf{v}\nabla)\mathbf{v} = \nabla p + \Delta \mathbf{v} + T\mathbf{k}, \quad (2)$$

$$\frac{\partial T}{\partial t} + Gr\mathbf{v}\nabla T = \frac{1}{Pr}\Delta T + \frac{F}{Pr}\exp T, \quad (3)$$

$$\nabla \mathbf{v} = 0, \quad (4)$$

where \mathbf{v} and p are the velocity and pressure, respectively, and \mathbf{k} is the unit vector in the positive z -direction. The flow is characterized by three dimensionless parameters: the Grashof number $Gr = \hat{g}\hat{\beta}R\hat{T}^2h^3/(\nu^2E)$, the Frank-Kamenetskii parameter $F = Q_0Eh^2/(\kappa R\hat{T}^2)\exp(-E/(R\hat{T}))$ and the Prandtl number $Pr = \nu/\chi$, where $\chi = \kappa/(\rho c_p)$, κ is the thermal conductivity, c_p is the specific heat. The Frank-Kamenetskii transformation is used to represent the source term in (3). Thus, there are two factors that induce convection: (a) internal heat sources (1) and temperature gradient across the layer due to difference in the temperatures of the walls.

These two factors generate a steady convective flow in the vertical direction. Equations (2)–(4) have a steady solution of the following form

$$\mathbf{v}_0 = (0, 0, v_0(x)), \quad T_0 = T_0(x), \quad p_0 = p_0(z). \quad (5)$$

Substituting (5) into (2)–(4) we obtain

$$v_0'' + T_0 = C, \quad (6)$$

$$T_0'' + F\exp(T_0) = 0, \quad (7)$$

where $C = dp_0/dz$ is a constant. The boundary conditions are

$$v_0(\pm 1) = 0, \quad (8)$$

$$T_0(\mp 1) = \pm 1. \quad (9)$$

The layer is assumed to be closed so that the total fluid flux through the cross-section is equal to zero:

$$\int_{-1}^1 v_0(x) dx = 0. \quad (10)$$

It is seen from (6)–(10) that the problem for the temperature distribution $T_0(x)$ can be solved independently. In the next section we consider solution of the boundary value problem for $T_0(x)$.

3 SOLUTION OF THE NONLINEAR BOUNDARY VALUE PROBLEM

Let F be a positive number. Consider the boundary value problem (7), (9). Let $T_0(x)$ be a solution of (7), (9). Then, $T_0''(x) = -F\exp(T_0(x)) < 0$ for every $x \in [-1, 1]$ and thus $T_0(x)$ is a strictly concave function in the interval $[-1, 1]$ and $T_0'(1) < 0$.

Let us consider the initial value problem (7),

$$T_0(1) = -1, \quad T'_0(1) = -\beta < 0. \quad (11)$$

It follows from (7), (11) that

$$T_0'^2(x) = \beta^2 + 2Fe^{-1} - 2Fe^{T_0(x)}. \quad (12)$$

Integrating (12), we have

$$\int_{-1}^{T_0(x)} \frac{du}{\pm \sqrt{\beta^2 + 2Fe^{-1} - 2Fe^u}} = x - 1, \quad (13)$$

where “+” sign is valid on intervals, where $T_0(x)$ increases and, consequently, “−” sign is for intervals, where $T_0(x)$ decreases.

Using formula 1.3.1.8 on p. 137 in [10], we obtain from (13) that

$$T_0(x) = \ln \left(\frac{4(\beta^2 + 2Fe^{-1})e^{-1+(x-1)\sqrt{\beta^2+2Fe^{-1}}}}{\left[\beta \left(-1 + e^{(x-1)\sqrt{\beta^2+2Fe^{-1}}} \right) + \sqrt{\beta^2 + 2Fe^{-1}} \left(1 + e^{(x-1)\sqrt{\beta^2+2Fe^{-1}}} \right) \right]^2} \right) \quad (14)$$

solves the initial value problem (7), (11). For T_0 defined by (14), $T'_0(x) = 0$ if and only if $x = x^*$, where

$$x^* = 1 + \frac{1}{\sqrt{\beta^2 + 2Fe^{-1}}} \ln \left(\frac{\sqrt{\beta^2 + 2Fe^{-1}} - \beta}{\sqrt{\beta^2 + 2Fe^{-1}} + \beta} \right).$$

Notice that $x^* < 1$. On account of (12), $T_0(x^*) = \max_{x \in \mathbb{R}} T_0(x) = \ln \left(\frac{2F + e\beta^2}{2eF} \right)$.

If $T_0(x)$ is defined by (14), then the equation $T_0(-1) = 1$ defines a bifurcation curve Γ in the positive quadrant of the (F, β) -plane which determine all solutions of the boundary value problem (7), (9). By calculations, $T_0(-1) = 1$ if and only if $G(F, \beta) = 0$, where

$$G(F, \beta) := 4e^{2(-1+\sqrt{\beta^2+2Fe^{-1}})}(\beta^2 + 2Fe^{-1}) - \left[\left(1 - e^{2\sqrt{\beta^2+2Fe^{-1}}} \right) \beta + \left(1 + e^{2\sqrt{\beta^2+2Fe^{-1}}} \right) \sqrt{\beta^2 + 2Fe^{-1}} \right]^2,$$

and thus $\Gamma = \{(F, \beta) \in \mathbb{R}^2 : F > 0, \beta > 0, G(F, \beta) = 0\}$; the curve Γ is depicted in Figure 1. Notice that $G(0, 1) = 0$. The curve Γ has a turning point $A_0 = (F_0, \beta_0) = (0.7887, 2.5363)$ (the brown point in Figure 1) from right to left. We conclude that the boundary value problem (7), (9) has exactly two solutions if $F \in (0, F_0)$, exactly one solution if $F = F_0$, and has no solutions if $F > F_0$.

Let us introduce the region $D := \{(F, \beta) \in \mathbb{R}^2 : F > 0, \beta > 0, x^* > -1\}$ and the curve $\Lambda := \{(F, \beta) \in \mathbb{R}^2 : F > 0, \beta > 0, x^* = -1\}$; see the shaded region and the black curve, respectively, in Figure 1. We mention some properties of solutions to (7), (9).

1. For the points $(F, \beta) \in \Gamma$ that are located in D , the corresponding solutions T_0 of (7), (9) have a maximum in the interval $[-1, 1]$, which is greater than one, and thus $T'_0(-1) > 0$; see Figure 2 and the blue solutions depicted in Figure 3, 4.
2. The curves Γ and Λ have a unique intersection point

$$A_2 = \left(\frac{1}{8e} \ln^2 \left(2e\sqrt{e^2 - 1} + 2e^2 - 1 \right), \frac{\sqrt{e^2 - 1}}{2e} \ln \left(2e\sqrt{e^2 - 1} + 2e^2 - 1 \right) \right);$$

see Figure 1. The solution T_0 of (7), (9) that corresponds to the point A_2 is strictly decreasing in the interval $[-1, 1]$ and $T'_0(-1) = 0$; see the green solution in Figure 3.

3. For the points $(F, \beta) \in \Gamma$ that are located outside of D and that are different from A_2 , the corresponding solutions T_0 of (7), (9) are strictly decreasing in the interval $[-1, 1]$ and $T'_0(-1) < 0$; see the green solution in Figure 4. We note that for such solutions T_0 the formula (12) should be used with “−” sign and $\int_{-1}^1 \frac{du}{\sqrt{\beta^2 + 2Fe^{-1} - 2Fe^u}} = 2$.

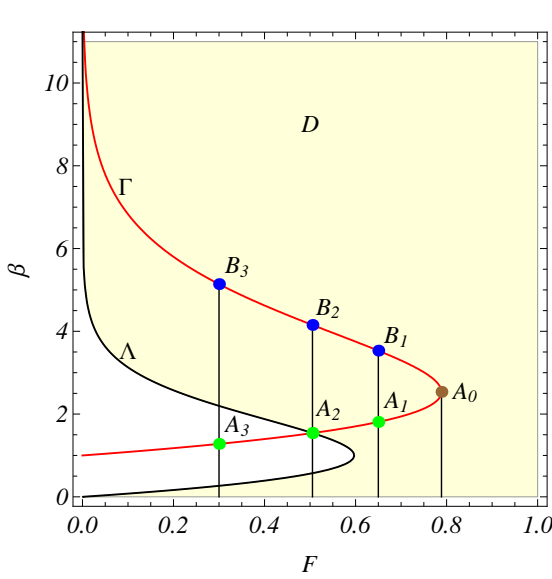


Figure 1: The bifurcation curve Γ (red).

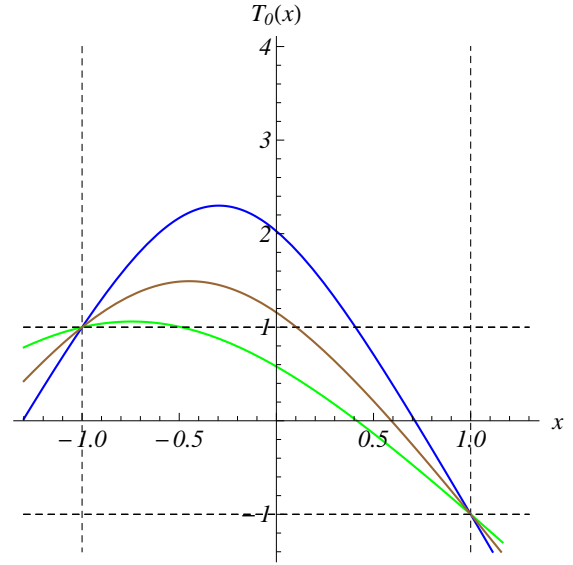


Figure 2: Three solutions of (7), (9) corresponding to the points $A_1 = (0.65, 1.8102) \in \Gamma$, $B_1 = (0.65, 3.5329) \in \Gamma$, and $A_0 = (0.7887, 2.5363) \in \Gamma$ depicted in Figure 1.

The results presented in this section allow one to select a physically realizable solution (corresponding to a point that is located on the lower branch of Γ), which is used later in linear stability analysis.

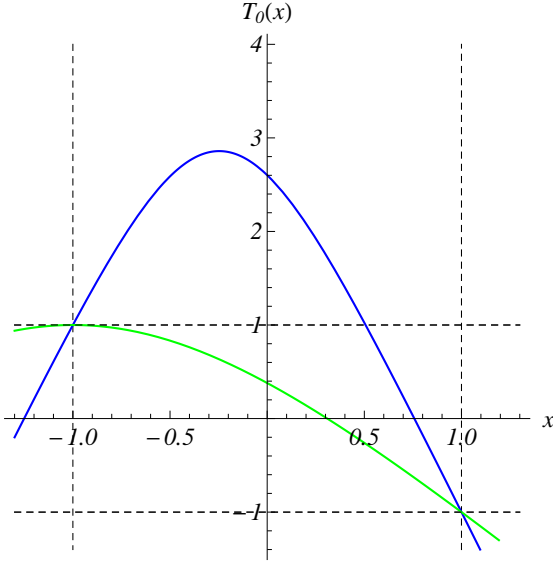


Figure 3: Two solutions of (7), (9) corresponding to the points $A_2 = (0.5053, 1.5412) \in \Gamma$ and $B_2 = (0.5053, 4.1538) \in \Gamma$ depicted in Figure 1.

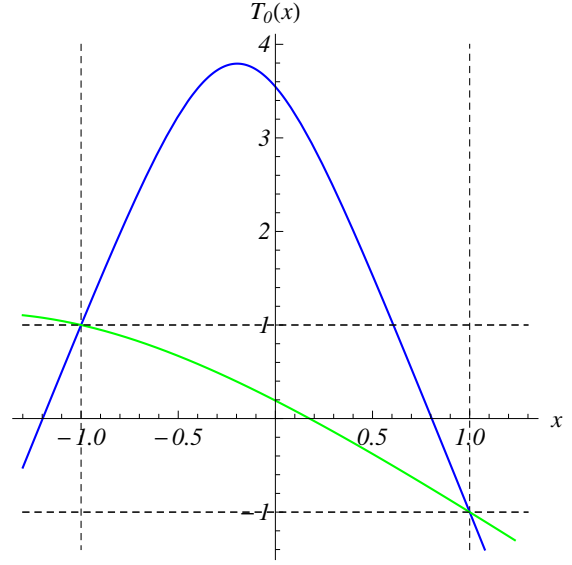


Figure 4: Two solutions of (7), (9) corresponding to the points $A_3 = (0.3, 1.2791) \in \Gamma$ and $B_3 = (0.3, 5.1406) \in \Gamma$ depicted in Figure 1.

4 LINEAR STABILITY ANALYSIS

Consider a perturbed flow of the form

$$\mathbf{v} = (0, 0, v_0(x)) + \mathbf{v}', \quad T = T_0(x) + T', \quad p = p_0(z) + p', \quad (15)$$

where flow quantities with primes represent small perturbations. Substituting (15) into (2)–(4), linearizing the resulting equations in the neighborhood of the base flow, introducing the normal modes

$$\psi' = \varphi(x)e^{-\lambda t + ikz}, \quad T' = \theta(x)e^{-\lambda t + ikz}, \quad (16)$$

where ψ' is the stream function for the perturbed velocity field and $\lambda = \lambda_r + i\lambda_i$ is a complex eigenvalue, we obtain the eigenvalue problem

$$\varphi^{(4)} - 2k^2\varphi'' + k^4\varphi + ikGr(\varphi v_0'' - v_0\varphi'' + k^2v_0\varphi) + \theta' = -\lambda(\varphi'' - k^2\varphi), \quad (17)$$

$$\frac{1}{Pr}(\theta'' - k^2\theta) + \frac{F}{Pr}e^{T_0}\theta + ikGr(\varphi T_0' - v_0\theta) = -\lambda\theta, \quad (18)$$

$$\varphi(\pm 1) = 0, \quad \varphi'(\pm 1) = 0, \quad \theta(\pm 1) = 0. \quad (19)$$

Problem (17)–(19) is solved by collocation method. The functions $\varphi(x)$ and $\theta(x)$ are approximated as follows

$$\varphi(x) = \sum_{n=0}^N a_n(1-x^2)^2 T_n(x), \quad \theta(x) = \sum_{n=0}^N b_n(1-x^2) T_n(x), \quad (20)$$

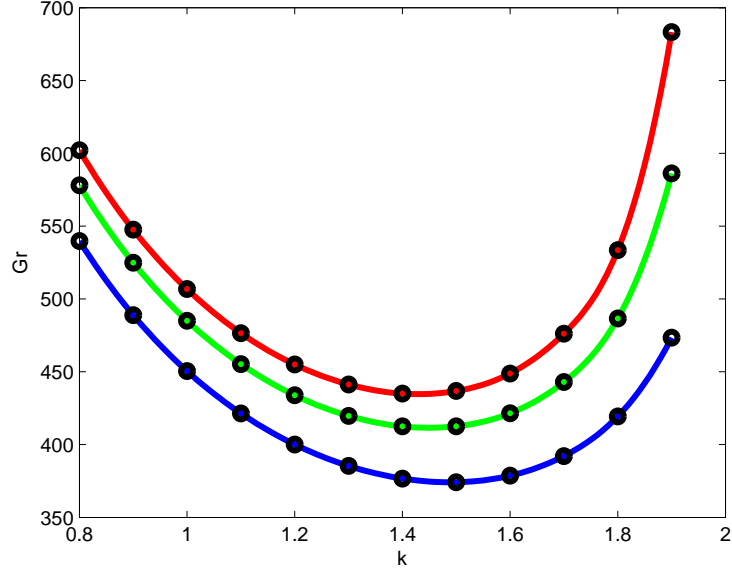


Figure 5: Marginal stability curves for $F = 0.3$ (red curve), $F = 0.5$ (green curve) and $F = 0.7$ (blue curve). The value of the Prandtl number is fixed at $Pr = 0.79$.

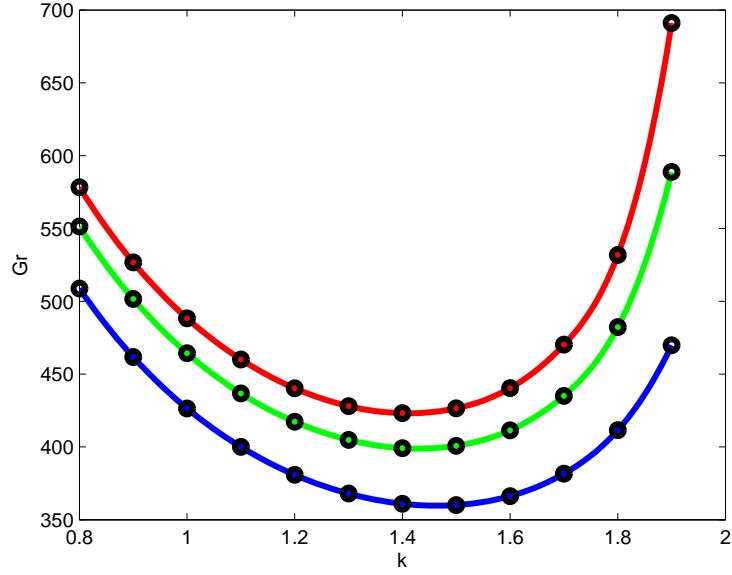


Figure 6: Marginal stability curves for $F = 0.3$ (red curve), $F = 0.5$ (green curve) and $F = 0.7$ (blue curve). The value of the Prandtl number is fixed at $Pr = 3$.

where $T_n(x)$ is the Chebyshev polynomial of the first kind of order n . The collocation points are

$$x_j = \cos \frac{\pi j}{N}, \quad j = 0, 1, \dots, n \quad (21)$$

Using (20), (21) we transform (17)–(19) to the generalized eigenvalue problem of the form

$$(A + \lambda B)\mathbf{a} = 0, \quad (22)$$

where $\mathbf{a} = (a_0 a_1 \dots a_n b_0 b_1 \dots b_n)^T$. Problem (22) is solved numerically in Matlab for different values of the parameters of the problem.

Marginal stability curves for the case $Pr = 0.79$ are shown in Fig. 5 for three values of the parameter F . Black points on each graph represent calculated values.

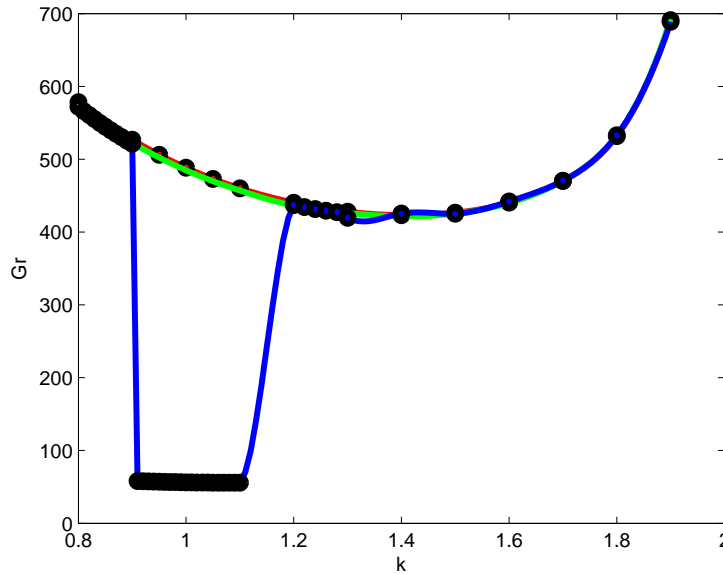


Figure 7: Marginal stability curves for $Pr = 3$ (red curve), $Pr = 10$ (green curve) and $Pr = 100$ (blue curve).

Calculated marginal stability curves for the case $Pr = 3$ are shown in Fig. 6. Comparing Figs. 5 and 6 we see that there are two destabilizing factors: the flow becomes less stable if the parameters F (the intensity of the chemical reaction) and Pr increase.

Another set of calculations is performed for the case $F = 0.3$ and three different Prandtl numbers. The results are plotted in Fig. 7. It is seen that for moderate range of the Prandtl numbers ($3 < Pr < 10$) the stability boundary is insensitive to the change in Pr (the red and green curves almost coincide in Fig. 7). For large Prandtl numbers ($Pr = 100$) the critical Grashof number decreases considerably. In addition, the most

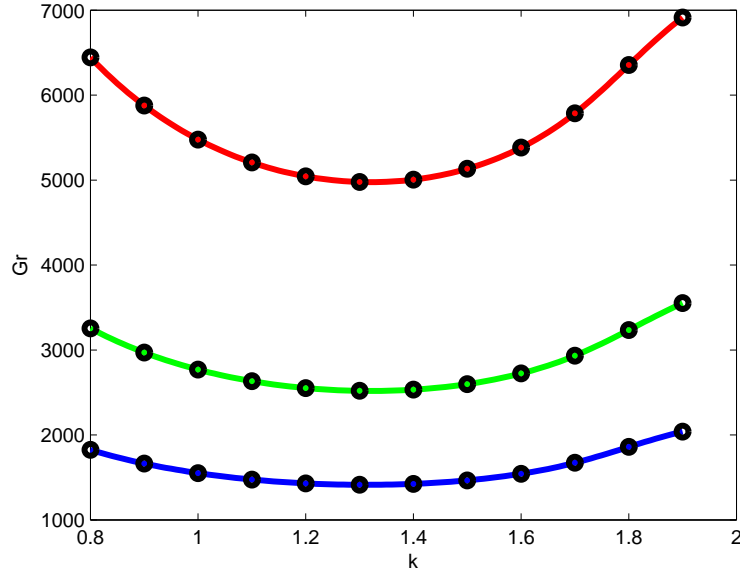


Figure 8: Marginal stability curves for $F = 0.3$ (red curve), $F = 0.5$ (green curve) and $F = 0.7$ (blue curve). The value of the Prandtl number is fixed at $Pr = 0.79$.

unstable mode in this case corresponds to perturbations with larger wave length (smaller wave numbers).

The graphs in Figs. 5–7 correspond to the case where there are two factors inducing convective flow: (a) internal heat generation and (b) constant dimensional temperature difference $2\hat{T}$ between the walls. Let us compare our results with the case where only factor (a) is present (both walls are maintained at equal and constant temperatures \hat{T} , see [8]). Marginal stability curves for the case $Pr = 0.79$ with equal wall temperatures are shown in Fig. 8. Comparing Figs. 5 and 8 we see that the presence of the temperature gradient between the walls considerably destabilizes the flow. In addition, the minimum of the marginal stability curve is shifted to the left in the (k, Gr) -plane. This means that perturbations of longer wavelength become more unstable as the Prandtl number grows.

5 CONCLUSIONS

Linear stability analysis of a steady flow of a chemically reacting fluid in a vertical layer bounded by two planes maintained at different constant temperatures is performed in the paper. Base flow solution is described by a nonlinear boundary value problem. The properties of this problem are investigated using bifurcation analysis. Results of linear stability calculations show that there are several destabilizing factors that affect linear stability: (a) the Prandtl number, (b) the Frank-Kamenetskii parameter. In addition, the presence of horizontal temperature gradient leads to considerable destabilization of the base flow in comparison with the case of equal temperatures of the walls.

6 ACKNOWLEDGMENT

This work was supported by the Latvian Council of Science, project No. lzp-2020/1-0076 “Analysis of complex dynamical systems in fluid mechanics and heat transfer”.

REFERENCES

- [1] Yamakawa, C.K., Qin, F. and Mussatto, S.I. Advances and opportunities in biomass conversion technologies and biorefineries for the development of bio-based economy. *Biomass and Bioenergy* (2018) **119**:54–60.
- [2] Lewandowski, W.M., Ryms, M. and Kosakowski, W. Thermal biomass conversion: a review. *Processes* (2020) **8**:doi:10.3390/pr8050516.
- [3] Barmina, I., Purmalis, M., Valdmanis, R. and Zake M. Electrodynamic control of the combustion characteristics and heat energy production. *Combustion Science and Technology* (2016) **188**:190–206.
- [4] Barmina, I., Valdmanis, R. and Zake M. The effect of biomass co-gasification and co-firing on the development of combustion dynamics. *Energy* (2018) **146**:4–12.
- [5] Kalis, H., Marinaki, M., Strautins, U. and Zake M. On numerical simulation of electromagnetic field effects in the combustion process. *Mathematical Modeling and Analysis* (2018) **23**:327–343.
- [6] Drazin, P.G. and Reid, W.H. *Hydrodynamic stability*. Cambridge University Press, (2004).
- [7] Schmid, P.J. and Henningson, D.S. *Stability and transition in shear flows*. Springer, (2001).
- [8] Eremin E.A. Stability of the stationary plane-parallel convective motion of a chemically active medium. *Fluid Dynamics* (1983) **18**:438–441.
- [9] Iltins, I., Iltina, M., Kolyshkin, A. and Koliskina, V. Linear stability of a convective flow in an annulus with a nonlinear heat source. *JP Journal of Heat and Mass Transfer* (2019) **18**:315–329.
- [10] Prudnikov, A.P., Brychkov Yu. A. and Marichev O.I. *Integrals and Series*. CRC, Vol. I., (1998).